Modeling Two Phase Fluid Flow in High Speed Countercurrent Chromatography

G. S. Flynn*, K. R. Weisbrod, R. M. Chamberlin, S. L. Yarbro
Los Alamos National Laboratory
*Corresponding author: garrison@lanl.gov

Abstract High-speed counter current chromatography (HSCCC) is a unique process presenting possibilities for efficient separations by creating a large interfacial area between two phases in countercurrent flow. Millifluidic channels rotate about both planetary and solar axes to create a rapidly changing gravitational field and unique flow patterns. This research seeks to further our understanding of the fluid dynamics of HSCCC through numerical simulation. A COMSOL Multiphysics model has been developed to study the behavior of the dynamic interface between two immiscible fluids using a two-phase laminar level set model subject to a dynamic gravitational field. The model simulates mixing of water and dodecane in a three layer 3.2 mm coil. Results indicate interface shape is governed by directional changes in tangential acceleration at alternatively low and high radial acceleration.

Keywords: j-type centrifuge, laminar flow, level set, liquid-liquid separation, millifluidics

1 Introduction

Liquid-liquid chromatography is a process for separation of components between two immiscible fluids. Separations take place in the form of mass transfer at the interface between the two phases. High speed countercurrent chromatography (HSCCC) is a particularly interesting method of liquid-liquid chromatography that leverages centrifugal and gravitational forces to rapidly mix and then separate the two phases.

HSCCC (also referred to as a J-type centrifuge) was first introduced by Ito (Ito et al. 1982, Ito and Conway 1986, Ito 1992) and has been through many design iterations, including helical columns where tubing is wrapped around a coil as well as a 2-dimensional spiral coil. The key to HSCCC operations is placement of the coil around a planetary axis which rotates around a solar axis, creating a cardioid rotational path (Figure 1). Through this type of rotation fluids in the column experience a rapidly changing centrifugal force. Additionally, the winding of the coil away from the planetary axis creates a gradient in gravitational forces along the column.

HSCCC may be operated in two modes: stationary retention and dual flow. When operating for stationary retention the column is filled with one phase while the other phase (i.e. the mobile phase) is pumped into the column. Mobile phase flows past the stationary phase due to pumping and gravitational forces. Dual flow involves continuously pumping the both phases into the column, with the heavy phase entering at the lower gravity end (column head) and the light phase entering at the higher gravity end (column tail), thus driving continuous countercurrent flow.

Wood et al. (2001, 2007) focused on derivation of centrifugal and gravitational forces to hypothesize the nature of mixing and settling in HSCCC. They developed mathematical models of the dynamic forces acting on the column. Theories on the forces governing mixing and settling regimes have been advanced as experimental imaging capabilities improve. For example, Guan et al. (2012) use stroboscopic illumination to image the two phases in a 2D spiral at different operating conditions. While informative, such experimental campaigns are not feasible for fully characterizing the fluid dynamics of HSCCC for implementation with new systems at varied conditions. Continued advancement of HSCCC technology requires numerical models capable of relating design and operating parameters to performance. In turn, these models will require rigorous validation with experimental data in order to confidently design new systems.

Initial efforts to develop such models are ongoing. He and Zhao (2007) empirically derive correlations of rotational speed and pumping flow rate to stationary phase retention. In their study He and Zhao demonstrate a general fit to data, but also demonstrate the variability in this fit given different liquid-liquid systems. König and Sutherland (2003) used computational fluid dynamics to model the wave patterns in a two phase closed system, first as a straight tube tilted at an angle and progressing to a closed ring followed by a three dimensional helix. These models provided the first insights to the nature of the mixing as waves formed due to the gravitational forces. These simulations were limited to 10 mm inner diameter tubing, leaving questions as to extrapolation of findings to smaller scale systems where viscous forces and pressure differences are more likely to influence mixing and settling behaviors. More recently, König and Sutherland (2007) expanded their CFD analysis to investigate mobile phase behavior at the point of injection in a 2D spiral with a 5 mm inner diameter.

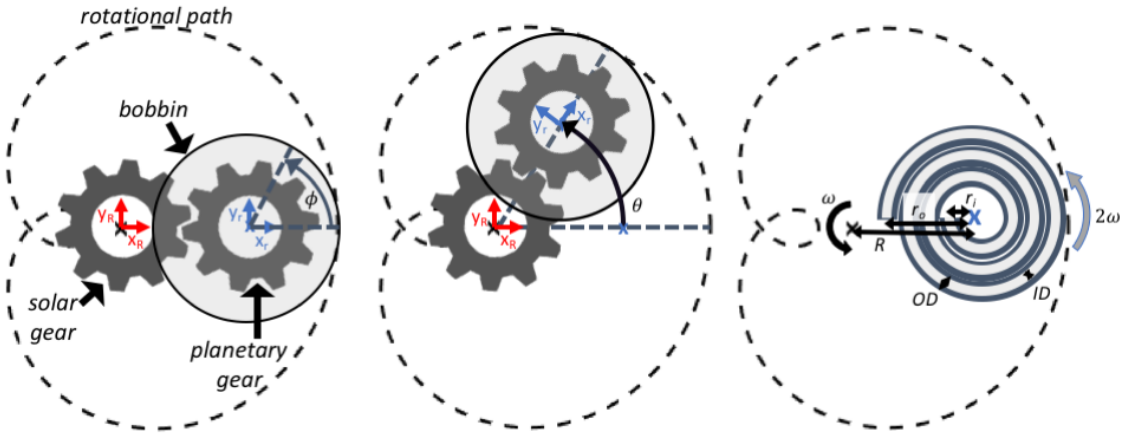

Figure 1. (a) HSCCC solar and planetary rotations resulting in cardioid motion. (b) Translation of planetary axes through rotation. (c) Parameterization of the column geometry.

Optimizing system design to enable continuous dual flow in HSCCC requires advancement of our current understanding on factors governing mixing and settling zones, particularly as columns are further scaled down to the millifluidic regime. Physics-based models incorporating all relevant design and operating parameters as well as physical properties of the fluids present a path forward for advancing our knowledge and guiding design optimization.

This paper presents a COMSOL Multiphysics model of the fluid dynamics in a three layer HSCCC with 3.2 mm inner diameter tubing. Mixing of water and dodecane is simulated under a dynamic, rotating gravitational forces. The goal of this work is to uncover physics-based relationships governing the mixing and settling regions of the column as well as the shape of the interface.

2 COMSOL Multiphysics Model

A fluid dynamics model has been developed in COMSOL Multiphysics to gain insight to the flow behaviors in a HSCCC device. HSCCC's fluid channels are contained by tubing typically a few millimeters (less than one inch) in diameter. Such small diameters maintain laminar flow in the system. Therefore, the laminar flow and level set modules were selected and coupled for the two-phase flow simulation.

Realistically the full column would be represented as a three dimensional helix where multiple layers wrap along the length of the bobbin. For simplicity this study considers a two dimensional slice of a coil with three layers. The inner diameter of the column is modeled as the fluid domain with separation of layers based on thickness of the tubing wall.

2.1 Parameterization

Ultimately the model will be used for design optimization. With this goal in mind the model was parameterized in three categories. First the geometry of the channel is parameterized based on conditions that can be modified by changing the gear size, bobbin core, and tubing sizes. Figure 1c relates these parameters to their physical meanings in the column geometry. Next, variable operating conditions are considered. Currently rotational speed is the only condition taken to be variable. However, flow rates for aqueous and organic feeds will be included as operational parameters as the modeling efforts are advanced to dual-flow operations. Finally, properties of the two phases are considered. The liquid-liquid system chosen for this study is water (aqueous) and dodecane (organic). Values of all model inputs are provided in Table 1.

Table 1: Model parameters.

Parameter	Value	Units
Geometric Parameters		
Solar radius, R	100	mm
Inner planetary radius, r_i	57.0	mm
Outer planetary radius, r_o	76.2	mm
Channel inner diameter, *ID*	3.20	mm
Channel outer diameter, *OD*	6.40	mm
Operational Parameters		
Rotational speed, ω	800	RPM
Fluid Properties		
Aqueous density, ρ_{aq}	1.00	g/cc
Aqueous viscosity, μ_{aq}	1.00	cP
Organic density, ρ_{org}	0.75	g/cc
Organic viscosity, μ_{org}	1.34	cP
Interfacial tension, σ_{int}	30.0	mN/m

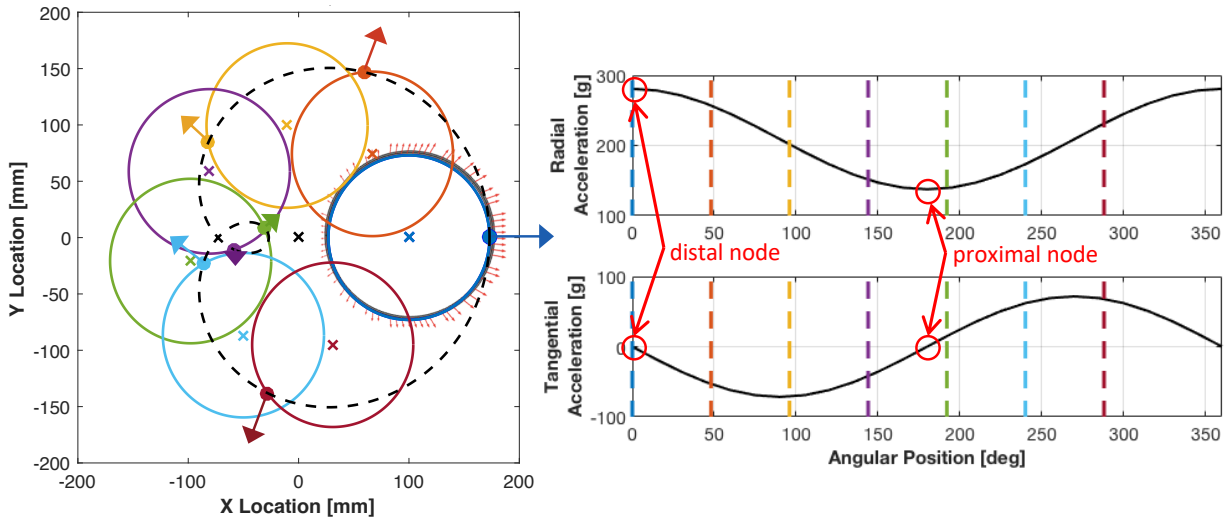

Figure 2. Radial and tangential accelerations during one full rotation about the solar axis at 800 RPM.

2.2 Rotating Gravitational Field

We are interested in modeling the fluid region of the column which is in constant motion both around the planetary and solar axes. Body forces due to acceleration from this motion are expected to cause the rapid mixing and separation between phases as well as the net movement of the light phase to the column head and heavy phase to the column tail. The model implemented herein keeps the fluid domain stationary with the forces dynamically changing as this reference frame is rotated.

Modeling the fluid domain as stationary requires derivation of the dynamic gravitational field. For this purpose let us define relevant coordinate systems. First is the coordinate system located at the center of the solar gear, x-y_R. This is the global coordinate system from which the rotational path and relative accelerations are derived. We also consider a local coordinate system based at the center of the planetary gear, x-y_r. This axis translates around the solar axis at a rate of ωt while also rotating about its centroid at a rate of $2\omega t$, where t represents time. Local coordinates are offset from x-y_r by an angle, ϕ, based on the initial position along the column.

$$\phi = \text{atan2}(y_r, x_r) \tag{1}$$

Initial locations of the coordinate systems are shown in Figure 1a and translations of the coordinate system during rotation are shown in Figure 1b.

Following derivations by Wood et al. (2001), the location of any point along the bobbin during rotation is determined by considering the solar rotational speed and radius, R, in conjunction with the planetary rotational speed and radius, r.

$$x_R = R\cos(\omega t) + r\cos(2\omega t + \phi) \tag{2}$$

$$y_R = R\sin(\omega t) + r\sin(2\omega t + \phi) \tag{3}$$

The solar radius, R, is constant. The planetary radius, r, changes along the length of the column as it winds from the inner to outermost layers. Substituting the radii ratio, β

$$\beta = \frac{r}{R} \tag{4}$$

and deriving acceleration with respect to the global coordinate system the gravitational forces, $a_{x,R}$ and $a_{y,R}$, are calculated.

$$a_{x,R} = -R\omega^2(\cos(\omega t) + 4\beta\cos(2\omega t + \phi)) \tag{5}$$

$$a_{y,R} = -R\omega^2(\sin(\omega t) + 4\beta\sin(2\omega t + \phi)) \tag{6}$$

Global accelerations in Equations 5 and 6 are translated to the local coordinate system so that the fluid domain may be modeled as physically 'stationary' with an equivalent gravitational acceleration changing relative to the true rotation. As seen in Figure 1b this local coordinate system is effectively the radial and tangential accelerations at any given point.

$$a_{x,r} = a_{x,R}\cos(2\omega t) + a_{y,R}\sin(2\omega t) \tag{7}$$

$$a_{y,r} = -a_{x,R}\sin(2\omega t) + a_{y,R}\cos(2\omega t) \tag{8}$$

Radial and tangential accelerations change for a given point in the bobbin during rotation. The point closest to the solar axis (proximal node) will have the lowest radial acceleration while the point furthest from the solar axis (distal node) will have the highest. The proximal and distal nodes are key to the fluid dynamics due to the change in direction of tangential acceleration at these points. Figure 2 illustrates radial

and tangential accelerations throughout the path of rotation for a single point on the bobbin.

Accelerations are applied to the fluids as body forces. The fluid domain is modeled as a cross-section of the bobbin centered at the planetary axis and physically stationary over time (x-y_r). Accelerations multiplied by relative fluid density, ρ, and applied to the fluid domain as body forces at each integration point in the model.

$$F_x = a_{x,r} \times \rho \quad (9)$$

$$F_y = a_{y,r} \times \rho \quad (10)$$

The resulting gravitational forces are therefore higher on the aqueous (heavy) phase and lower on the organic (light) phase.

2.3 Two Phase Level Set

Level set module is used to track the distribution of the two phases and the moving interface between them. As the fluids redistribute in the column the physical properties at each integration point are recalculated based on the phase variable, ϕ, which is equal to 0 for the organic phase, 1 for the aqueous phase, and linearly interpolates across the interface.

$$\rho = \rho_1 + (\rho_2 - \rho_1)\phi \quad (11)$$

$$\mu = \mu_1 + (\mu_2 - \mu_1)\phi \quad (12)$$

Updating the density is particularly important due its influence on the gravitational forces applied to the fluid.

2.4 Boundary Conditions

This study focuses on the effects of centrifugal and gravitational forces. As such, pumping of aqueous and organic feeds is neglected and the model represents a closed system. The closed system is modeled by a no flow boundary conditions along the walls as well as at the head and tail of the column. A no slip boundary is assumed for the laminar flow along the tubing walls (Figure 3).

2.5 Initial Conditions

Without continuous pumping of aqueous and organic feeds the HSCCC system will never truly reach a steady-state condition, rather, aqueous will also be moving towards the tail and likewise organic will be pushed to the head. Although this model is a closed system with no feeds being pumped into the coil, our goal is to represent the full process as closely as possible. Within the column the most common state of the fluids should be an even distribution of aqueous and organic along the length. For this reason we wish to start the simulation with a even distribution of phases throughout the column.

To maintain the most physically realistic initial condition we first model the coil with the phases loaded opposite of their gravitational preference (i.e. aqueous loaded at the head and organic loaded at the tail) with an equal volume ratio of each phase. Fluids are initially at rest. Rotation is ramped from 0 to 800 RPM over a 0.1 s interval and held at 800 RPM for 5 seconds. After this point the fluids have begun flowing towards the opposite ends of the column creating a relatively even distribution along the column length. Rotation speed is then ramped down from 800 RPM to 0 RPM over a 0.1 s interval and held stationary at 0 RPM for 5 seconds. This time period after rotation had stopped allows the fluids to settle into a distribution representative of that in a column that has been evenly loaded but not yet operated. Distribution of fluids in the stationary column is predominately governed by interfacial tension.

The two phases are found to separate into small bands evenly distributed along the column length. This distribution is used for all continuing studies as the initial condition with fluids at rest, as shown in Figure 3. Such a banded initial distribution is thought to be a realistic representation of a column that is loaded with both phases simultaneously and left to settle based on interfacial forces before HSCCC operations. The full simulation begins with the coil initially at rest and ramps to full rotational speed over 0.15 s.

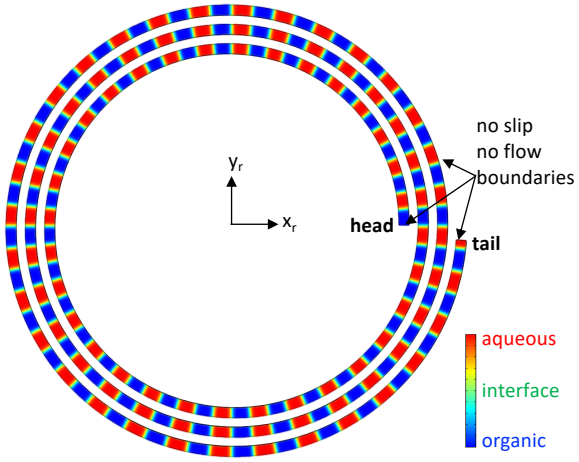

Figure 3. Initial and boundary conditions.

2.6 Finite Element Mesh

The fluid domain is meshed with mapped quad elements. The mesh is confined such that there are ten elements across the inner diameter of the tubing and twelve elements along the length of each different phase segment. The resulting mesh is composed of 23,040 quad elements with a minimum element quality of 0.9857.

3 Results and Discussion

The key to rapid mixing and settling is found to be the change in tangential acceleration which occurs alternatively at high and low radial acceleration, as seen in Figure 4. Snapshots in Figure 4 are selected such that the bottom and top are always the proximal and distal nodes, respectively. At different points in the process a wave like interface is seen on the left side of the coil while a smoother interface is observed on the right side of the coil. These results indicate a consistency in the onset of waves (mixing) due to the change of the direction of tangential force at low radial force (proximal node) while the change of direction in tangential force at high radial force (distal node) causes the interface to flatten (separation). Tracking a single point in the column along its cardioid path and considering the relevant acceleration changes we can concur that the two phases are being mixed and then separated at any given point once per rotation, meaning 800 mix/separation steps per minute in the current simulation.

Formation and suppression of this wave motion is further captured in Figure 5 which shows the top of the outermost layer of the coil through a single solar

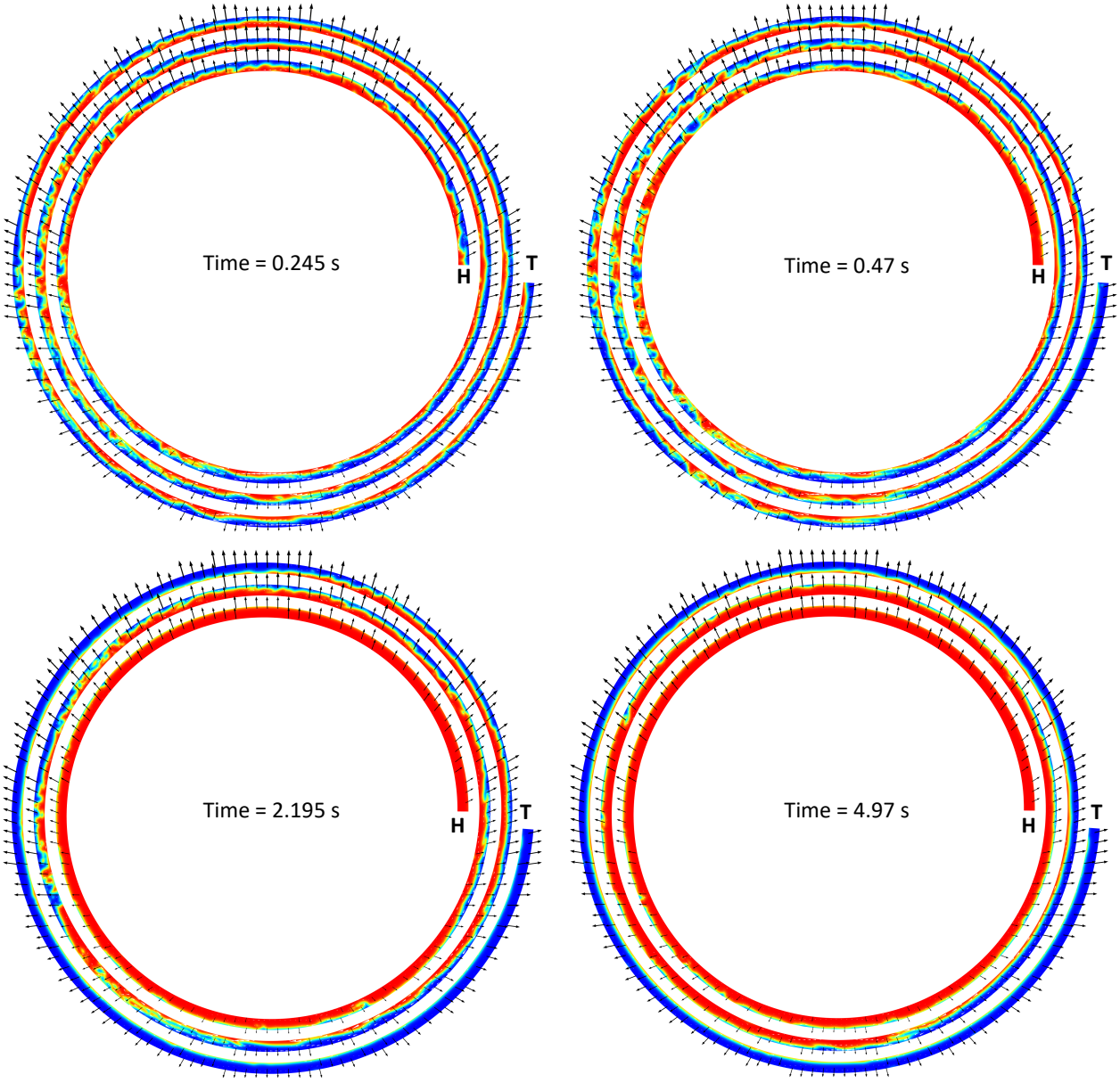

Figure 4. Distribution of phases over time with mixing initiated at the proximal node and separation initiated at the distal node. Over time aqueous (blue) collects in the tail (T) and organic (red) collects in the head (H).

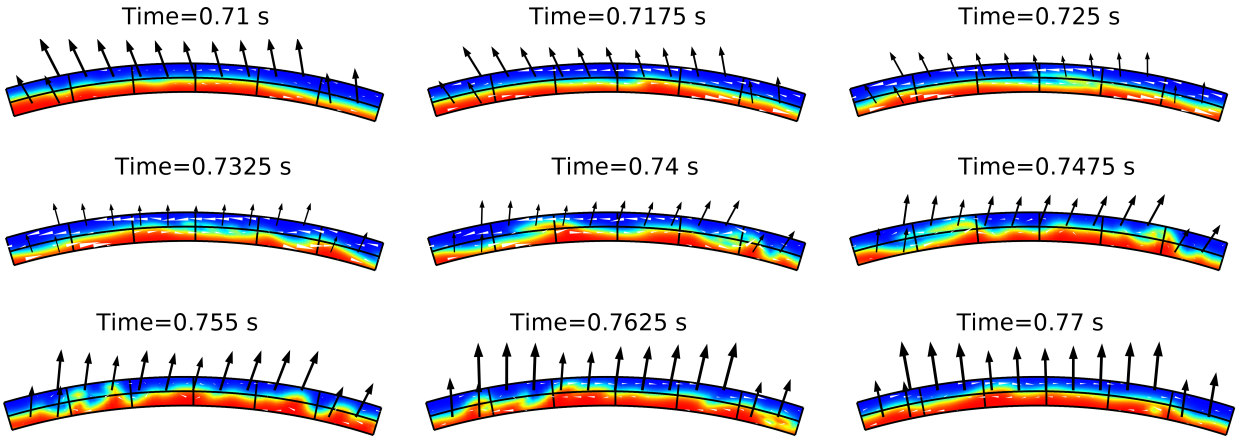

Figure 5. Transitions of wave pattern with body forces shown by back arrows and fluid velocity shown by white arrows.

rotation. We observe the aqueous (being the heavier phase) staying on the outer edge of the coil. Fluids are passing through the proximal node at t = 0.7325s and passing through the distal node at t = 0.77s. The gravitational force is rotating counterclockwise. Aqueous and organic phases are found to be flowing countercurrent to one another at the highest relative velocities during the transition period from distal to proximal node. At the proximal node the velocities begin to accelerate in the opposite direction. This change in direction causes the phases to back up onto themselves and create the wavelike interface until passing back through the distal node. The fluids have a slight delay in responding to the directional change in force due to the fluid's inertia. Despite changing directions, fluid velocities never reach the same magnitude in the

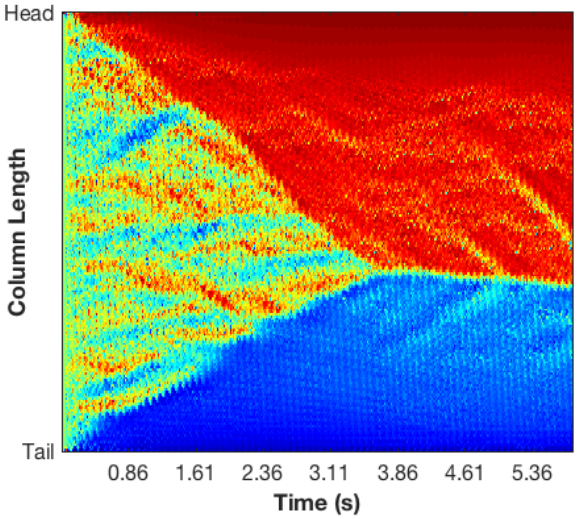

Figure 6. Distribution of phases across the column length beginning with an even mix throughout the whole length and ending with organic (red) contained in the head and aqueous (blue).

mixed flow as they do the separated flow. This discrepancy in velocity magnitude between the two flow directions creates an internal pumping force pushing the heavy phase in the direction it flows in the separation region.

Together, the pumping action and the gravitational difference from head to tail work to force the aqueous and organic phases to flow past one another eventually separating with aqueous in the tail and organic filling the head. Figure 6 illustrates the progression of the column from fully mixed to nearly separated. In this figure the length of the coil is represented linearly from head to tail along the y-axis with simulation time on the x-axis. Color represents the average phase across the diameter of the column at the given point in space and time, meaning that the fully red areas are 100% organic while the fully blue are 100% aqueous. Green regions represent a 50/50 mix of aqueous and organic along the cross section.

4 Conclusion

Two-phase laminar flow modeled with COMSOL Multiphysics has been used to better understand the governing forces of HSCCC. The physics based model has provided insights to the nature of mixing and settling in a millifluidic HSCCC system. Interface tracking through the level set module revealed wavelike interface generated and suppressed every rotation due to the unique changes in gravitational force.

Results obtained thus far provide valuable insight, however, many assumptions require further investigation. Accuracy of the no slip boundary condition around column walls decreases with tubing diameter and should become a function of the fluid wetting properties with the tubing material. Continuous pumping of aqueous and organic feeds

will be implemented in future models to better represent true operations.

Ultimately, furthering knowledge on relationships between column design parameters and performance is critical for achieving optimized, stable flows in these devices. In future work the model will serve as a baseline for parametric studies and design optimization.

5 References

1. Y.H. Guan, R. van del Heuvel, Y.P. Zhuang, Visualization of J-type Counter-current Chromatography: A Route to Understand Hydrodynamic Phase Distribution and Retention, *Journal of Chromatography*, **1239**:15, 10-21 (2012).
2. C.H. He and C.X. Zhao, Retention of the Stationary Phase for High-Speed Countercurrent Chromatography, *AIchE Journal*, **53:** 6, 1460-1471 (2007).
3. Y. Ito and J. Sandlin, High-speed Preparative Counter-current Chromatography with a Coil Planet Centrifuge, *Journal of Chromatography*, **244**:2, 247-258 (1982).
4. Y. Ito and W. Conway, High-speed Countercurrent Chromatography, *Analytical Chemistry*, **17**:1, 65-143 (1986).
5. Y. Ito, Speculation on the Mechanism of Unilateral Hydrodynamic Distribution of Two Immiscible Solvent Phases in the Rotating Coil, *Journal of Liquid Chromatography,* **15**:15-16, 2639-2675 (1992).
6. C.S. König and I.A. Sutherland, An Investigation of the Influence of the Gravity Field on the Interface of Two Immiscible Liquids – A Computational Study Comparing Prediction with Experiment, *Journal of Liquid Chromatography,* **26**:9-10, 1521-1535 (2003).
7. P. Wood, B. Jaber, I.A. Sutherland, A New Hypothesis on the Hydrodynamic Distribution of the Upper and Lower Phases in CCC, *Journal of Liquid Chromatography,* **24**:11-12, 1629-1654 (2001).
8. P. Wood, B. Jaber, L. Janaway, N. Terlinden, I.A. Sutherland, Effect of β-Value on the Head and Tail Distribution of the Upper and Lower Phases in Helical Coils, *Journal of Liquid Chromatography,* **28**:12-13, 1819-1837 (2007).